

Experimental and theoretical investigations of the EFG parameters at the Br site in Cd(BrO₃)₂·2H₂O

R. Valli and K. V. S. Rama Rao

Citation: *The Journal of Chemical Physics* **79**, 4113 (1983); doi: 10.1063/1.446360

View online: <http://dx.doi.org/10.1063/1.446360>

View Table of Contents: <http://scitation.aip.org/content/aip/journal/jcp/79/9?ver=pdfcov>

Published by the [AIP Publishing](#)

Articles you may be interested in

[Experimental and theoretical studies of the O\(3P\) + C₂H₄ reaction dynamics: Collision energy dependence of branching ratios and extent of intersystem crossing](#)

J. Chem. Phys. **137**, 22A532 (2012); 10.1063/1.4746758

[Preparation and investigation of the A-site and B-site terminated SrTiO₃\(001\) surface: A combined experimental and theoretical x-ray photoelectron diffraction study](#)

J. Appl. Phys. **112**, 073505 (2012); 10.1063/1.4757283

[Experimental and theoretical investigation on the high frequency dielectric properties of Ag/Al₂O₃ composites](#)

Appl. Phys. Lett. **99**, 032903 (2011); 10.1063/1.3608156

[Experimental and theoretical investigation of the autoionization dynamics in the excited collision complex He*\(23S\)+H\(12S\)](#)

AIP Conf. Proc. **295**, 852 (1993); 10.1063/1.45255

[ESR study of Cd\(BrO₃\)₂·2H₂O single crystals \$\gamma\$ irradiated at 300 and 77 K](#)

J. Chem. Phys. **82**, 639 (1985); 10.1063/1.448965



Experimental and theoretical investigations of the EFG parameters at the Br site in $\text{Cd}(\text{BrO}_3)_2 \cdot 2\text{H}_2\text{O}$

R. Valli and K. V. S. Rama Rao

Department of Physics, Indian Institute of Technology, Madras 600 036, India
(Received 10 February 1983; accepted 15 April 1983)

In $\text{Cd}(\text{BrO}_3)_2 \cdot 2\text{H}_2\text{O}$ there are two chemically inequivalent sites of bromine in the unit cell which give rise to two nuclear quadrupole resonances for each isotope of bromine both at RT as well as at LNT. Single crystal Zeeman experiments carried out on the ^{79}Br resonances at RT have revealed the presence of four physically inequivalent sites belonging to each crystallographic site of bromine and the EFG parameters at these sites have been obtained. The conventional point-charge model, when applied to this system for the evaluation of the field gradient at the Br sites, has yielded unsatisfactory results. In an attempt to include the effect of the covalent bonding in the bromate group, CNDO/2 MO calculations have been carried out on the two inequivalent bromate groups of the system and from the resulting population densities in the orbitals, intraionic EFG or q_{cov} has been estimated. Later, interionic contribution q_{ion} , obtained from a point-charge approximation to the rest of the lattice has been added to q_{cov} to obtain the total EFG. The results obtained from this model are in good agreement with the experimental values and it is found that intraionic EFG forms more than 95% of the total EFG at the Br site.

INTRODUCTION

In the bromate salts, the bromine atom is present in the molecular ion $(\text{BrO}_3)^-$ and is covalently bonded to the oxygens of the group, whereas the whole lattice is ionic. The electric field gradient (EFG) at the bromine site can be considered to be made up of two parts: The contribution coming from the particular $(\text{BrO}_3)^-$ group that contains the resonant atom (intraionic) and the contribution coming from the rest of the ions in the lattice (interionic). The nuclear quadrupole resonance (NQR) frequency of bromine in all the bromates that have been studied so far¹ lies in a narrow frequency range and this range is intermediate between the NQR frequency of bromine in a typical ionic solid and a molecular solid. Similar grouping of resonance frequencies is found also in the case of chlorine resonances in chlorates.^{2,3} This fact suggests that the EFG at the halogen site in chlorates or bromates is mainly due to the $\text{XO}_3(\text{X}=\text{Cl}, \text{Br})$ ion. The theoretical calculation of EFG carried out so far on chlorates and bromates⁴⁻⁶ is based on the point-charge approximation to the entire lattice and this model has not been successful in all the cases.

In the present investigation an attempt has been made to investigate the relative importance of the intraionic and interionic EFG's at the bromine site in $\text{Cd}(\text{BrO}_3)_2 \cdot 2\text{H}_2\text{O}$. First, the conventional point-charge model has been applied to the lattice and as expected the results have not been satisfactory. Later, the intraionic EFG of the bromine group has been determined separately, taking into consideration the covalent bonding in the group. For this purpose CNDO/2 molecular orbital (MO) calculations have been carried out on the $(\text{BrO}_3)^-$ ions of this system. Finally, the interionic contribution obtained from a point-charge approximation to the rest of the lattice has been added to the intraionic EFG to give the total EFG. For comparison with the theoretical values, the EFG parameters at the Br site have been determined experimentally from single crystal Zeeman effect studies.

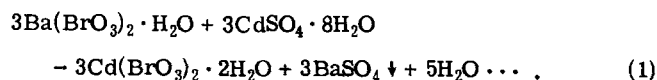
CRYSTALLOGRAPHY

The crystal structure of $\text{Cd}(\text{BrO}_3)_2 \cdot 2\text{H}_2\text{O}$ has been reported recently by two independent groups.⁷⁻⁹ The crystal belongs to the orthorhombic system and the space group is $P2_12_12_1 (D_2^2)$. The structure data given by both the groups are nearly the same, but for an interchange in the naming of "b" and "c" axes and a shift in the origin in fixing the position coordinates. The unit cell contains^{7,8} four molecular units and its dimensions are $a = 12.492 \text{ \AA}$, $b = 6.170 \text{ \AA}$, and $c = 9.328 \text{ \AA}$. The projection of the crystal structure in the c plane is given in Fig. 1. The bromine atom occupies two crystallographically inequivalent sites in the unit cell. The atoms Br(1), O(11), O(12), and O(13) form one bromate group whereas Br(2), O(21), O(22), and O(23) form the other bromate group. In bromate group (1) the Br-O bond lengths are in the range 1.65–1.70 \AA and the O-O bond lengths are in the range 2.57–2.67 \AA . In bromate group (2) the Br-O bond length varies from 1.63 to 1.68 \AA and the O-O bond length varies from 2.58 to 2.63 \AA . It has been postulated^{7,8} that hydrogen bond may exist between $\text{H}_2\text{O}(1)$ molecule and O(11) and O(22). Similarly, $\text{H}_2\text{O}(2)$ molecule may have hydrogen bonds with O(13) and O(23).

EXPERIMENTAL

A. Preparation of the material and crystal growth

$\text{Cd}(\text{BrO}_3)_2 \cdot 2\text{H}_2\text{O}$ was obtained by double decomposition of $\text{Ba}(\text{BrO}_3)_2 \cdot \text{H}_2\text{O}$ and $3\text{CdSO}_4 \cdot 8\text{H}_2\text{O}$:



A hot solution of $\text{Ba}(\text{BrO}_3)_2 \cdot \text{H}_2\text{O}$ in water is mixed with an aqueous solution of $3\text{CdSO}_4 \cdot 8\text{H}_2\text{O}$. Since $\text{Cd}(\text{BrO}_3)_2 \cdot 2\text{H}_2\text{O}$ is highly soluble in water, it appears in solution, whereas BaSO_4 precipitates out. The precipitate is filtered out and the solution is heated to evaporate water. The material obtained is purified

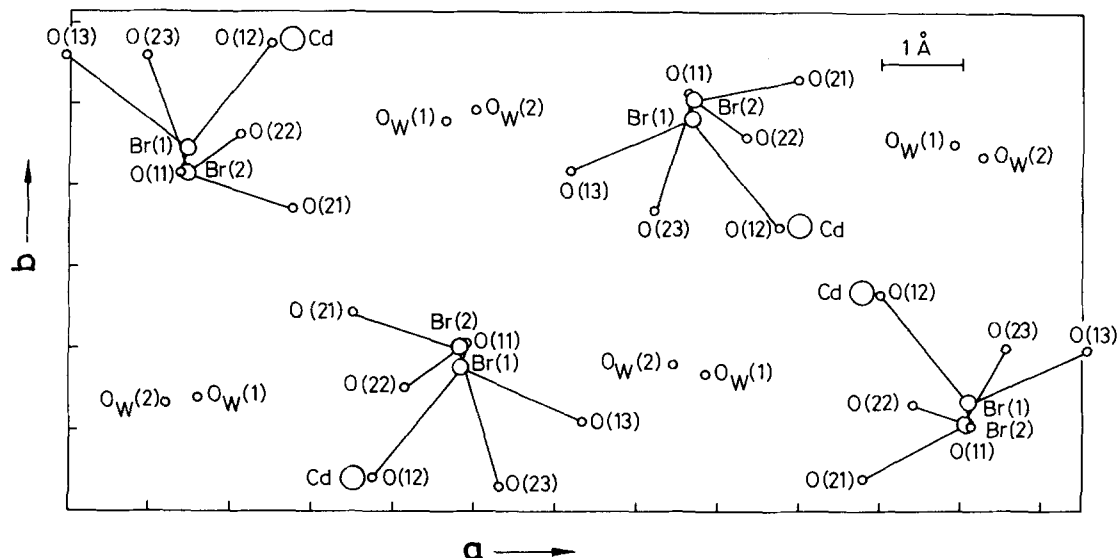


FIG. 1. Crystal structure of $\text{Cd}(\text{BrO}_3)_2 \cdot 2\text{H}_2\text{O}$. Projection in the c plane.

by recrystallization from water. Cadmium bromate is known to exist as monohydrate as well as dihydrate. Thermogravimetric analysis (TGA) done on the sample revealed that the substance obtained is dihydrate.

Good and large single crystals required for Zeeman study were grown from saturated aqueous solution at room temperature.

B. Identification of the faces in the crystal for Zeeman study

The morphology of the crystal has been described by Groth.¹⁰ The ratio $a : b : c$ given by Groth is 0.9885 : 1 : 0.7392. If this if a is halved and interchanged with b , the ratio obtained agrees with the x-ray data. When this change is made in Groth's data, the indices of the most prominent faces will be given as $\{100\}$, $\{101\}$, $\{011\}$, and $\{021\}$. The long axis of the crystal is c axis. These faces have been observed by examining tiny crystals under optical goniometer.

For conducting Zeeman effect studies of nuclear quadrupole resonance, large single crystals are required and the crystals used in the present work are more than 2 cm^3 in size. Since optical goniometer cannot be used with such big crystals, the interfacial angles between the different faces have been measured with contact goniometer and the faces identified. In order to confirm these identifications, Laue photographs and single crystal diffractograms have been taken for certain specific directions.

C. Detection of NQR signals and arrangement of crystal holder and Zeeman coil

An externally quenched superregenerative oscillator detector has been employed for the detection of NQR signals.

For conducting the Zeeman effect studies, a pair of Helmholtz coils capable of producing uniform magnetic

field has been employed. The separation of the coils is 18 cm and the field produced at the center is nearly 30 G/A. A maximum current of 5 A has been used. The coil can be rotated about a vertical axis in the horizontal plane. This rotation varies the polar angle " θ " of the magnetic field with respect to the crystal fixed coordinate system that is chosen as the reference. The crystal holder, used for holding the crystal in position inside the horizontal tank coil, can be rotated about the horizontal axis in the vertical plane. This rotation varies the azimuthal angle ϕ of the magnetic field orientation. The angles θ and ϕ have been measured to an accuracy of $\pm 0.5^\circ$.

D. Method of analysis

For the determination of EFG parameters the method of zero-splitting locus¹¹ has been employed. The angle ϕ is kept fixed at intervals of 5° and θ is varied continuously from 0° to 180° and the points of coalescence of the α and α' components are noted. Similarly θ is kept fixed at regular intervals and ϕ is varied to obtain the zero-splitting points. The points obtained are plotted on a stereographic net and the zero-splitting loci are traced.

EXPERIMENTAL RESULTS

A. Pure quadrupole resonance studies

In $\text{Cd}(\text{BrO}_3)_2 \cdot 2\text{H}_2\text{O}$ two resonances have been observed for each isotope of bromine both at RT as well as at 77 K and the frequencies are listed in Table I. The ^{79}Br NQR spectrum obtained with polycrystalline sample at RT is shown in Fig. 2. From the Zeeman effect experiments, the results of which will be described in the following section, it is found that the higher frequency line (line 1) at RT corresponds to the bromine atom referred to as Br(1) in the structure while the other line (line 2) corresponds to the Br(2) atom.

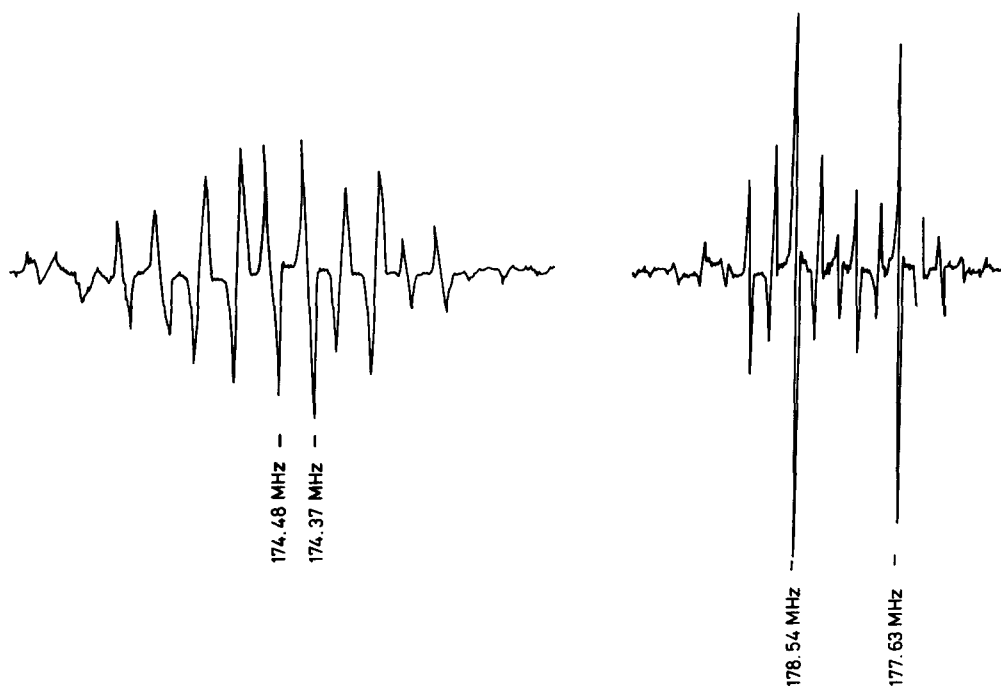


FIG. 2. ^{79}Br NQR spectrum in a polycrystalline sample of $\text{Cd}(\text{BrO}_3)_2 \cdot 2\text{H}_2\text{O}$ at (a) 305 K and (b) 77 K.

B. Zeeman effect studies

Zeeman effect studies have been conducted for two different orientations of the crystal. In the first orientation the c axis of the crystal was chosen as the "z" axis of the crystal fixed coordinate system xyz and the crystal was mounted with this axis parallel to the radio frequency (rf) axis. The a axis was chosen as the "x" axis. The ^{79}Br NQR spectrum obtained in this arrangement of the crystal is shown in Fig. 3. The resonances from both the crystallographic sites have good signal-to-noise ratio and the Zeeman splitting of both the lines have been studied. Figure 4 shows the zero-splitting loci obtained for Br(1) resonance in this rotation (rotation I). The portions of the loci near the edges are not shown in the plot. There are four loci A , B , C , and D showing that these are four different orientations of the EFG tensor corresponding to this site. In other words, there are four physically inequivalent Br(1) sites in the unit cell. Figures 5(a) and 5(b) show the zero-splitting loci E , F , G , and H obtained for the resonance due to Br(2). Here also there are four physically inequivalent sites. The data obtained have been analyzed and the direction cosines of the principal EFG z axis and the

asymmetry parameter η at these sites have been determined. The results are given in Table II.

The experiment was repeated by rotating the crystal about the a axis. The c axis of the crystal was taken as the x axis of the crystal fixed coordinate system xyz . The NQR spectrum of ^{79}Br obtained when the crystal is arranged in this way is shown in Fig. 6. In this orientation the intensity of the resonance from the Br(2) site is too low to study the splittings and hence the experiment has been carried out only on the resonance from the Br(1) site. The zero-splitting loci obtained for this line in this rotation (rotation II) is shown in Fig. 7. The portions of the loci near the edges are not shown in the plot. There are four loci A' , B' , C' , and D'

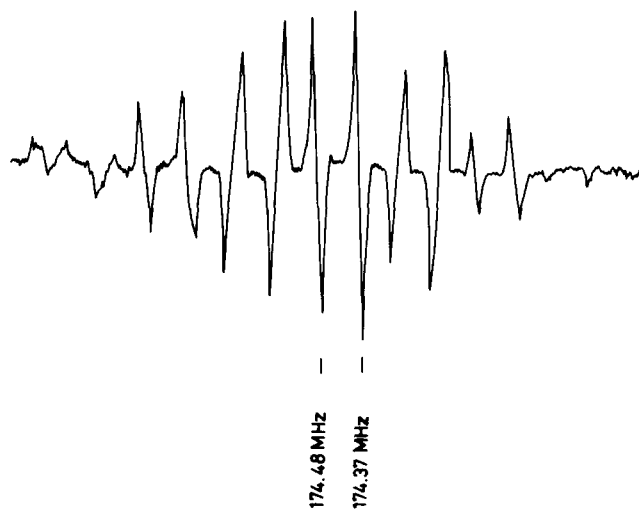


FIG. 3. ^{79}Br NQR spectrum in single crystal of $\text{Cd}(\text{BrO}_3)_2 \cdot 2\text{H}_2\text{O}$ oriented with c axis parallel to rf axis.

TABLE I. NQR frequencies of bromine in $\text{Cd}(\text{BrO}_3)_2 \cdot 2\text{H}_2\text{O}$.

Site	Temperature (K)	NQR frequency of	
		^{79}Br (MHz)	^{81}Br (MHz)
Br(1)	305	174.48	145.76
	77	177.63	148.39
Br(2)	305	174.37	145.67
	77	178.54	149.16

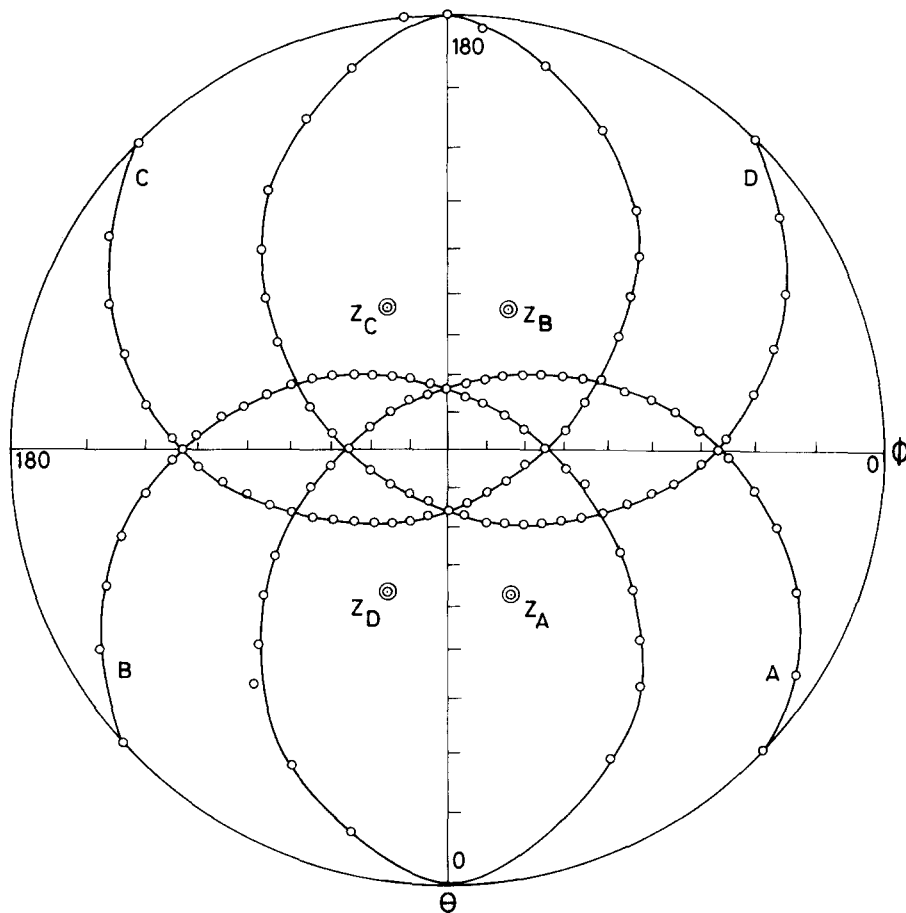


FIG. 4. Stereographic plot of the loci *A*, *B*, *C*, and *D* obtained for line one in rotation I.

which correspond, respectively, to the loci *A*, *B*, *C*, and *D* obtained in rotation I. The EFG parameters derived from these loci are shown in Table III.

THEORETICAL EVALUATION OF THE EFG PARAMETERS

A. Calculations based on the point-charge model

In the conventional point-charge model the point charge approximation is used for the entire lattice including the atoms that are covalently bonded to the resonant atom. In an idealized model the ions in the lattices are assumed to be spherically symmetric having a closed shell structure and the coupling constant is written as

$$e^2qQ = (e^2qQ)_{\text{latt}}(1 - \gamma_{\infty}), \quad (2)$$

where $(e^2qQ)_{\text{latt}}$ is obtained by summing up the contributions of the various ions in the lattice. γ_{∞} is the anti-shielding factor.

In the present work, the lattice summations have been computed using a program written for IBM 370/155 system. This program can be used for calculating the EFG in crystals belonging to cubic, tetragonal, orthorhombic, and also monoclinic systems.

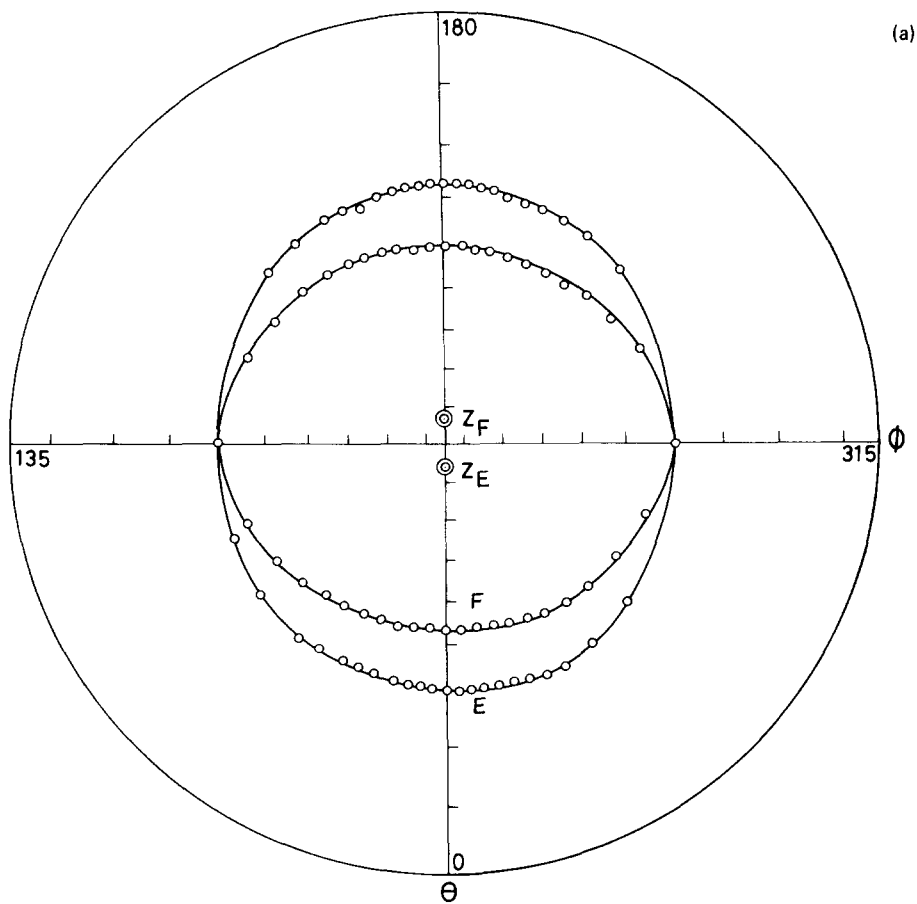
Regarding the charges assigned to the various atoms, complete ionicity has been assumed and a charge of $+2e$ and $-e$ have been assigned to the cadmium atom and the bromate group, respectively, where e is the proton charge. The water molecule has been assumed to be replaced by a charge of $+0.3e$ on the protons and

TABLE II. EFG parameters obtained from rotation I.

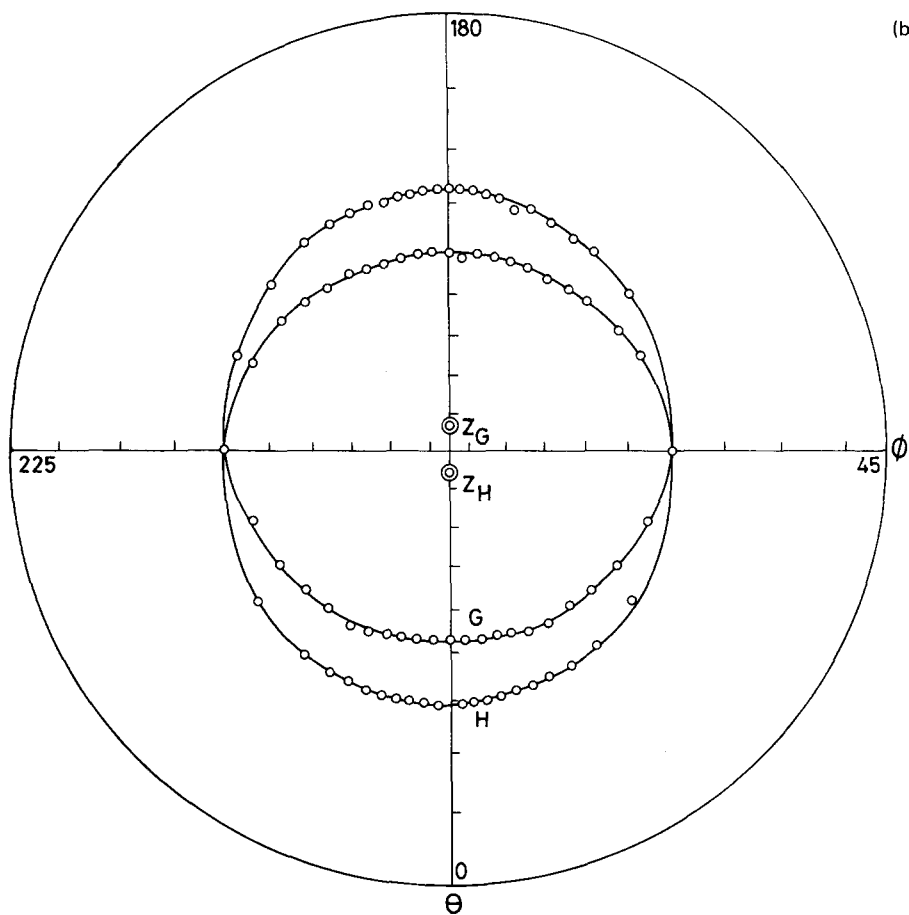
Site	Locus	Direction cosines of the <i>Z</i> axis with respect to			
		<i>a</i>	<i>b</i>	<i>c</i>	η
Br(1)	<i>A</i>	0.2505	0.7733	0.5824	0.05
	<i>B</i>	0.2439	0.7752	-0.5826	0.05
	<i>C</i>	-0.2549	0.7710	-0.5834	0.05
	<i>D</i>	-0.2451	0.7707	0.5882	0.05
Br(2)	<i>E</i>	0.7085	0.6975	0.1072	0.03
	<i>F</i>	0.7044	0.6982	-0.1278	0.02
	<i>G</i>	-0.7053	0.6987	-0.1201	0.02
	<i>H</i>	-0.7070	0.6999	0.1009	0.01

TABLE III. EFG parameters obtained from rotation II.

Site	Locus	Direction cosines of the <i>Z</i> axis with respect to			
		<i>a</i>	<i>b</i>	<i>c</i>	η
Br(1)	<i>A'</i>	0.2923	0.7671	0.5676	0.06
	<i>B'</i>	0.2923	0.7778	-0.5528	0.04
	<i>C'</i>	-0.2756	0.7777	-0.5650	0.05
	<i>D'</i>	-0.2924	0.7587	0.5822	0.05



(a)



(b)

FIG. 5. (a) Stereographic plot of the loci E and F obtained for line two in rotation I. (b) Stereographic plot of the loci G and H obtained for line two in rotation I.

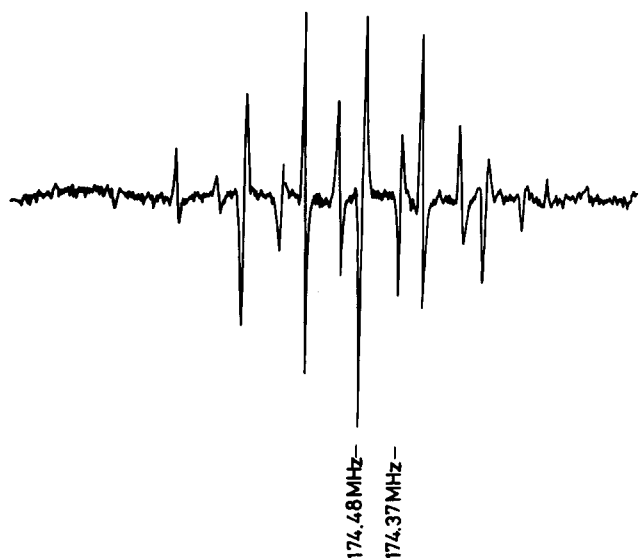


FIG. 6. ^{79}Br NQR spectrum in single crystal of $\text{Cd}(\text{BrO}_3)_2 \cdot 2\text{H}_2\text{O}$ oriented with a axis parallel to rf axis.

a charge of $-0.6e$ on the oxygen, consistent with the value of the dipole moment of water. The positions of the hydrogens have been deduced from the postulated hydrogen bonds taking $\text{O}_w\text{-H}$ bond distance to be 0.987 \AA . From the CNDO/2 MO calculations done on the two inequivalent bromine groups of this system, the details of which follow, the net charges on bromine and oxygens

have been deduced. The charges obtained are

$\text{Br}(1): 0.3270e$, $\text{O}(11): -0.4502e$,

$\text{O}(12): -0.4544e$, and $\text{O}(13): -0.4244e$

and

$\text{Br}(2): 0.3289e$, $\text{O}(21): -0.4464e$,

$\text{O}(22): -0.4273e$, and $\text{O}(23): -0.4553e$.

These charges have been substituted in the point-charge model calculations.

Having fixed the charges on all the different types of ions, the summation of their contributions is carried over successive shells of unit cells until satisfactory convergence of all the components of the EFG tensor is reached. The EFG tensor thus obtained in the abc axes system is then diagonalized to obtain the principal components. The EFG parameters obtained for the $\text{Br}(1)$ and $\text{Br}(2)$ sites are shown in Table IV. The quadrupole coupling constant (QCC) has been evaluated substituting the various values of γ that are available in the literature¹²⁻¹⁶ for Br .

B. Intraionic EFG based on MO calculations

As mentioned already in the Introduction, the EFG at the Br site can be considered as the sum of the intra-ionic EFG or the covalent EFG q_{cov} and the other contribution coming from the rest of the ions in the lattice, which may be referred to as the interionic EFG or q_{ion} . Thus, $q = q_{\text{cov}} + q_{\text{ion}}$.

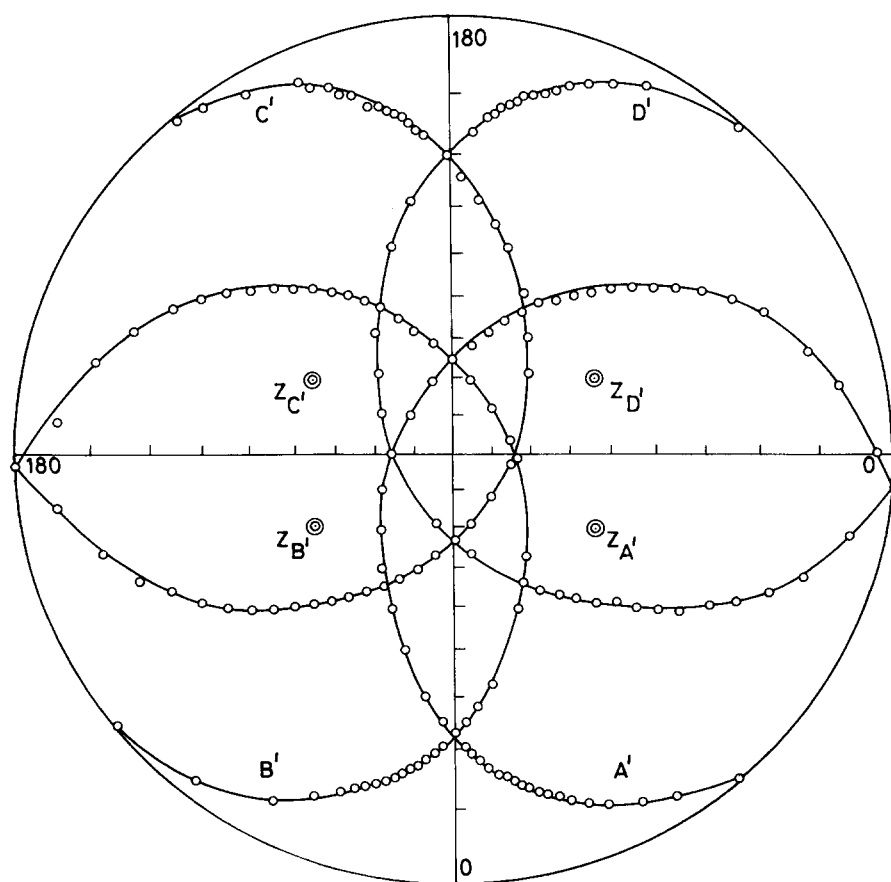


FIG. 7. Stereographic plot of the loci A' , B' , C' , and D' obtained for line one in rotation II.

TABLE IV. Results of the point-charge model calculations compared with the experimental values.

Site	Quantity	Experimental			Theoretical		
					γ_{∞}	$ e^2qQ/h $ (MHz)	
Br(1)	$ e^2qQ/h $ in MHz	349.24			-35 ^a	50.8	
					-99 ^b	141.1	
					-123 ^c	174.9	
					-195 ^d	276.5	
					-210 ^e	297.7	
η	0.05			0.46			
Direction cosines of Z axis with respect to: a b c axes	-0.25	0.77	-0.58	-0.02	0.62	-0.78	
Br(2)	$ e^2qQ/h $ in MHz	348.79			-35	69.2	
					-99	192.4	
					-123	238.6	
					-195	377.1	
					-210	406.0	
η	0.02			0.29			
Direction cosines of Z axis with respect to: a b c axes	0.71	0.70	0.11	0.65	0.67	0.35	

^aReference 16.^bReference 12.^cReference 13.^dReference 15.^eReference 14.

In the present investigation, in order to determine the intraionic EFG, MO calculations based on the CNDO/2 scheme have been performed on the two inequivalent bromate groups of Cd(BrO₃)₂ · 2H₂O. The method of Cotton and Harris¹⁷ as adapted by Kaplansky and Whitehead¹⁸ has been used for the determination of EFG.

A computer program¹⁹ to do numerical calculations based on the CNDO/2 scheme for atoms not heavier than chlorine is already available. For the present work, this program has been extended to III row atoms along the line of Hase and Schweig.²⁰ When III row atoms are present, Coulomb and exchange integrals will involve the 4s, 4p, and 4d orbitals also and this necessitates the addition of a few more y and z coefficients in the program. The parameters of the CNDO/2 method required for the III row atoms have been taken to be the same as those prescribed in Ref. 20.

The configurations of the groups are taken to be the same as those given in the x-ray data. The 4s, 4p, and 4d orbitals of bromine and 2s and 2p orbitals of the three oxygens have been considered in the basis set. Once the molecular orbitals have been determined as linear combination of atomic orbitals (LCAO's) as

$$k = \sum_{i=1}^n C_i^k \phi_i \quad (3)$$

the population density matrix is constructed. The population density matrix is, in general, a square matrix whose order is equal to the number of orbitals in the basis set. The elements of this matrix are of the general form

$$P_{ij} = 2 \sum_k^{\text{occ}} C_i^k C_j^k, \quad (4)$$

where the summation is over all the occupied MOs. Since only the P electrons of the resonance atom have the maximum contribution to the various terms in the population density matrix, the 3 × 3 submatrix on the p orbitals of the resonant atom alone is important in the determination of EFG. These population density submatrices obtained for the two bromate groups are shown in Table V.

When the MOs have been obtained following the CNDO scheme, the approximations involved in Cotton and Harris method¹⁷ become imperative and in addition the

TABLE V. Population density submatrices in abc system.

(a)-Br(1) site			
	P_x	P_y	P_z
P_x	0.9326	-0.0547	0.0604
P_y	-0.0547	1.1894	-0.2017
P_z	0.0604	-0.2017	1.0995
(b)-Br(2) site			
	P_x	P_y	P_z
P_x	1.1163	0.2086	0.0367
P_y	0.2086	1.1292	0.0417
P_z	0.0367	0.0417	0.9015

TABLE VI. Comparison of the EFG parameters obtained from intraionic EFG with the experimental values.

Site	Quantity	Experimental				Theoretical	
	$ e^2qQ/h $ in MHz	349.24				337.46	
Br(1)	η	0.05				0.11	
	Direction cosines of Z axis with respect to: <i>a b c</i> axes	-0.25	0.77	-0.58	-0.18	0.76	-0.62
	$ e^2qQ/h $ in MHz	348.79				334.27	
Br(2)	η	0.02				0.07	
	Direction cosines of Z axis with respect to: <i>a b c</i> axes	0.71	0.70	0.11	0.69	0.71	0.13

terms involving differential overlap also vanish. Hence, the principal field gradient at the site of an atom say α , is reduced to a simple expression of the form

$$(eq)_\alpha = \{P_{zz} - \frac{1}{2}(P_{xx} + P_{yy})\}(eq)_{e1}, \quad (5)$$

where P_{xx} , P_{yy} , and P_{zz} are the electron populations in the P_x , P_y , and P_z orbitals of the atom α and $(eq)_{e1}$ is the principal component of the field gradient due to a single electron in the P_x orbital of free atom α . Cotton and Harris, in their method, have made an additional assumption that the MOs have been derived in the principal axes system of the EFG tensor and hence Eq. (5) can be readily employed only in those cases where the principal axes system is known *a priori*. For the other cases where the MOs have been obtained with any arbitrary coordinate system as the reference, the elegant method suggested by Kaplonsky and Whitehead¹⁸ may be used. Using hydrogenlike wave functions for the atomic orbitals, and following the same approximations as in Ref. 17, Kaplonsky and Whitehead have derived expressions for all the six nonidentical components of the EFG tensor. While the diagonal terms are of the same form as in Eq. (5), the off-diagonal terms are obtained as

$$q_{xy} = \frac{3}{2}P_{xy}(eq)_{e1}. \quad (6)$$

From Eq. (6), it is clear that when the off-diagonal terms of the population density matrix vanish, the off-diagonal terms of the EFG tensor also vanish. Therefore, Kaplonsky and Whitehead suggested that diagonalization of the population density matrix takes one from the reference coordinate system to the principal axes system of the EFG.

Following this method, the population density matrices shown in Table V have been diagonalized. The eigenvectors give the direction cosines of the EFG axes with respect to the reference axes (*abc*) system. From the eigenvalues the principal components of the EFG tensor are calculated using the expressions given in Eq. (5). The principal axes have been named *X*, *Y*, and *Z* such that $|q_{xx}| \leq |q_{yy}| \leq |q_{zz}|$. The asymmetry parameter η is obtained from

$$\eta = \frac{q_{xx} - q_{yy}}{q_{zz}}. \quad (7)$$

The quadrupole coupling constant is obtained from

$$e^2qQ = \{P_{zz} - \frac{1}{2}(P_{xx} + P_{yy})\}(e^2qQ)_{e1}, \quad (8)$$

where $(e^2qQ)_{e1}$ for Br is -759.756 MHz.²¹ The results obtained from these calculations are shown in Table VI. It can be seen that for both Br(1) and Br(2) sites, all the three parameters are very close to the corresponding experimental values.

C. Addition of the interionic EFG to the intraionic EFG

The results that are described in the preceding section show that the intraionic EFG or q_{cov} forms a major part of the total EFG at the Br site in $\text{Cd}(\text{BrO}_3)_2 \cdot 2\text{H}_2\text{O}$. However, there is a small contribution from the ions in the rest of the lattice which must be added to the intraionic EFG to obtain the total EFG. This method of clubbing the covalent contribution with the ionic contribution has been followed by a few workers in the past.²²⁻²⁴

Brill *et al.*²² and Maurer *et al.*,²⁴ while combining the interionic EFG and molecular EFG, have directly added the principal components of the two EFGs. This is strictly valid only if the principal axes system of the two EFGs coincide. Since this has not been found to be the case in the present calculations, the two EFGs have been added in the *abc* system itself.

The interionic EFG has been obtained on the basis of the simple point-charge approximation to the rest of the lattice. From the EFG obtained using the conventional point-charge model calculations (which is in the *abc* system), the contributions due to the point charges situated at the oxygen sites of the particular bromate group have been subtracted and this gives the EFG due to the rest of the ions in the lattice. The interionic EFG thus obtained is multiplied by a $(1 - \gamma_\infty)$ factor to account for the additional contribution that will be introduced consequent of the deformation caused by the extraionic charges, in the core and the valence electron distribution of Br. Of the different values of γ_∞ reported for Br, three values -35 , -99 , and -123 have been used.

To obtain the components of the intraionic EFG in the *abc* axes system, the population density submatrices

TABLE VII. EFG parameters obtained from the addition of intraionic and interionic contributions compared with the experimental values.

	$ (e^2 q Q/h) $ (MHz)	η	Direction cosines ^a		
Br(1) site					
Experimental	349.24	0.05	-0.25	0.77	-0.58
Theoretical					
(i) $\gamma_\infty = -35$	326.46	0.05	-0.15	0.80	-0.59
(ii) $\gamma_\infty = -99$	315.07	0.11	-0.08	0.85	-0.52
(iii) $\gamma_\infty = -123$	313.50	0.17	-0.06	0.86	-0.50
Br(2) site					
Experimental	348.79	0.02	0.71	0.70	0.11
Theoretical					
(i) $\gamma_\infty = -35$	330.34	0.07	0.70	0.71	0.06
(ii) $\gamma_\infty = -99$	333.54	0.09	0.70	0.71	-0.05
(iii) $\gamma_\infty = -123$	337.97	0.18	0.70	0.71	-0.09

^aThe direction cosines are with respect to a , b , and c axes of the crystal.

shown in Table V have been used without diagonalization. Expressions of the type given in Eqs. (5) and (6) give the diagonal and off-diagonal elements of the tensor, respectively. Tensorial matrices of the interionic EFG and intraionic EFG are then added to obtain the total EFG in the abc axes system. This is then diagonalized to derive the values of the required EFG parameters. Table VII gives the results obtained.

DISCUSSION

The stereogram in Fig. 8 shows the directions of the Z axes obtained experimentally, for the different Br sites in the unit cell. The space group $P2_12_12_1$ is a noncentro symmetric group and the different physically inequivalent sites are obtainable from one another by the application of the three nonintersecting twofold rotations which are the symmetry operations of the group. Since the directions of the principal field gradient axes are not affected by translation, the directions of the EFG axes at these sites must be related by the twofold rotations about the a , b , and c axes. From Fig. 7, it is clear that the directions of the Z axes that have been obtained from the experiment obey this symmetry.

Point-charge model calculations done in the past²⁵ have shown that the model is capable of predicting the directions of the EFG axes reasonably well, provided the correct geometry has been assumed. In the present investigation also this has been found to be true. As far as the coupling constants derived from point-charge model are concerned, the agreement or disagreement cannot be easily judged because of the uncertainty in the value of γ_∞ . However, it is noteworthy that in the present case, large values of γ_∞ in the range of -200 , are required to bring the coupling constants obtained from point-charge model, close to the experimental values.

For both the Br sites, the values of the asymmetry parameter η given by the point-charge model calcula-

tions are very much higher than the corresponding experimental values. The determination of η does not involve γ_∞ and hence is free from any uncertainty. Therefore, the agreement or disagreement observed in the value of γ_∞ can be taken as a measure of the success or failure of the point-charge model. Judging from this, it is clear that for the system under study, the conventional point-charge model is not successful.

On the other hand, when the covalent contribution from the particular bromate group (intraionic EFG) alone is considered the theoretical parameters agree very well with the experimental values.

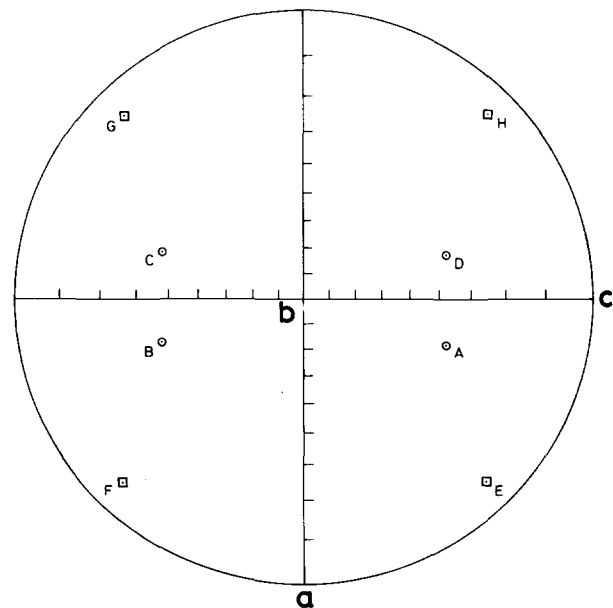


FIG. 8. Stereogram showing the directions of the principal field gradient Z axes at the bromine sites in $\text{Cd}(\text{BrO}_3)_2 \cdot 2\text{H}_2\text{O}$. Circles correspond to Br(1) sites and squares correspond to Br(2) sites.

The QCCs derived from intraionic EFG are less than the corresponding experimental values only by about 4%. The difference between the QCCs for the two sites, predicted by theory is nearly 3 MHz, while the experimental value at RT is less than 1 MHz. But it should be remembered that in the theoretical determination of the coupling constants, the motional averaging of the EFG has not been taken into account. The asymmetry parameters derived from these calculations are also higher than the corresponding experimental values but the agreement is far better than that obtained from the point-charge model. The direction cosines of the Z axes are also found to be much closer to the experimental values.

The fact that the QCCs that have been derived from the intraionic EFG are less than the corresponding experimental values only by a narrow margin proves that the main contribution to the EFG at the Br site comes from the corresponding bromate group. As far as the method adopted for the determination of intraionic EFG is concerned, in spite of its approximate nature, the method has yielded reasonably good results. Sichel and Whitehead²¹ have already used the CNDO approximation for the determination of coupling constants in a number of small compounds like HCl, HBr, HI, NH_3 , etc., and have observed that CNDO/2 method is well suited for the determination of QCC of halogens. The parametrization followed in the present work is along the lines of Hase and Schweig²⁰ and is not the same as that used by Sichel and Whitehead.²⁶ Hase and Schweig²⁰ have obtained the parameters from the optimization of bond lengths, bond angles, ionization potentials, and dipole moments and this method of parametrization is along the lines of the original CNDO/2 parametrization.²⁷ To our knowledge, the present work is the first case where the extension suggested in Ref. 20 has been used for the determination of EFG and from the present results, it may be believed that this extension²⁰ is capable of yielding correct values of QCCs.

In $\text{Cd}(\text{BrO}_3)_2 \cdot 2\text{H}_2\text{O}$ there may be hydrogen bonding between the water molecules and the atoms of the bromate group. This bonding may to some extent, influence the electron population in the orbitals of the resonant atom. However, this effect could not be included in the present MO calculations, due to the non-availability of data on the exact positions of the hydrogen atoms. The overlap effect of the bromine atom with the neighboring metal atom also has not been considered. However, the bromate salts are known to be highly ionic and therefore the neglect of this effect is not likely to affect the results seriously.

Finally, coming to the addition of the interionic EFG to the molecular EFG, it is seen that the addition has not produced marked improvement over the results obtained purely from intraionic EFG. The addition of the lattice contribution has reduced the values of QCCs from the corresponding intraionic values, thus taking them further away from the experimental values. The reason for this may be that, the effect of induced moments is appreciable in this case and that the lattice contribution obtained from simple point-charge approximation

to the rest of the lattice is incorrect. This may be so, because in a few cases studied in the past, it has been observed that, the effect of the induced moments is so high that, the inclusion of them changes even the sign of the coupling constant.

If the variation of the EFG parameters with change in γ_∞ values is examined, it is interesting to note that for $\gamma_\infty = -35$, the EFG parameters obtained are closer to the experimental values than those obtained for $\gamma_\infty = -99$ and $\gamma_\infty = -123$, with the QCC obtained for the Br(2) site, being the only exception. This observation indicates that the values of γ_∞ for Br present in $(\text{BrO}_3)^-$ group may be around -35 and not as high as -99 or -123 .

In conclusion, the following may be stated. From the present theoretical and experimental investigation on $\text{Cd}(\text{BrO}_3)_2 \cdot 2\text{H}_2\text{O}$, it has become clear that in bromates, of the contribution to the total EFG at any Br site, that due to the bromate group comprising the particular Br site is of prime importance and is constituting more than 95% of the total contribution. Any model in which this intraionic contribution is computed realistically, considering the covalent effects present in the group, is in all respects far superior to the conventional point-charge model. This will be true for all the systems in which the resonant atom is situated in a polyatomic group.

ACKNOWLEDGMENTS

The authors are thankful to Dr. M. S. Gopinathan for the help in MO calculations. One of the authors (RV) is grateful to the University Grants Commission and Seethalakshmi Ramaswami College, Trichy, for granting fellowship under Faculty Improvement Programme.

- ¹S. L. Segel and R. G. Barnes, Catalogue of N. Q. interactions and resonance frequencies in solids, USAEC Report IS-520, Part I.
- ²R. Moshier, Inorg. Chem. **3**, 199 (1964).
- ³P. U. Sakellariadis and C. A. Kagarakis, J. Mol. Struct. **14**, 127 (1972).
- ⁴R. Bersohn, J. Chem. Phys. **29**, 326 (1958).
- ⁵R. A. Bernheim and H. S. Gutowsky, J. Chem. Phys. **32**, 1072 (1960).
- ⁶J. Ramakrishna, Indian J. Pure Appl. Phys. **4**, 435 (1966).
- ⁷V. V. Satyanarayana Murty and B. V. R. Murty, Z. Kristallogr. Kristallgeom. Kristallphys. Kristallchem. **148**, 158 (1978).
- ⁸V. V. Satyanarayana Murty, Ph.D. thesis, Indian Institute of Technology, Madras, 1980.
- ⁹N. I. Golovastikov, Sov. Phys. Crystallogr. **24**, 135 (1979).
- ¹⁰P. Groth, *Chemische Kristallographie* (Von Wilhelm, Engelmann, 1917), Vol. 2.
- ¹¹T. P. Das and E. L. Hahn, Solid State Phys. Suppl. **1**, 11 (1958).
- ¹²E. G. Wikner and T. P. Das, Phys. Rev. **109**, 360 (1958).
- ¹³R. M. Sternheimer, Phys. Rev. **132**, 1638 (1963).
- ¹⁴F. D. Feiock and W. R. Johnson, Phys. Rev. **187**, 39 (1969).
- ¹⁵K. D. Sen and P. T. Narasimhan, *Advances in NQR*, edited by J. A. S. Smith (Heyden, London, 1974), Vol. 1.
- ¹⁶G. Burns and E. G. Wikner, Phys. Rev. **121**, 155 (1961).
- ¹⁷F. A. Cotton and C. B. Harris, Proc. Natl. Acad. Sci. U.S.A.

- A 56, 12 (1966).
- ¹⁸M. Kaplansky and M. A. Whitehead, *Trans. Faraday Soc.* **65**, 641 (1969).
- ¹⁹J. A. Pople and D. L. Beveridge, *Approximate MO Theory* (McGraw-Hill, New York, 1970), Appendix A.
- ²⁰H. L. Hase and A. Schweig, *Theor. Chim. Acta* **31**, 215 (1973).
- ²¹J. M. Sichel and M. A. Whitehead, *Theor. Chim. Acta* **11**, 263 (1968).
- ²²T. B. Brill, Z. Z. Hugus, Jr., and A. F. Schreiner, *J. Phys. Chem.* **74**, 469 (1970).
- ²³P. Morgen and W. W. Filho, *J. Chem. Phys.* **62**, 2183 (1975).
- ²⁴H. M. Maurer, P. C. Schmidt, and A. Weiss, *J. Mol. Struct.* **41**, 111 (1977).
- ²⁵K. V. Raman, R. Jaganathan, and P. T. Narasimhan, *J. Chem. Phys.* **59**, 792 (1973), and references therein.
- ²⁶J. M. Sichel and M. A. Whitehead, *Theor. Chim. Acta* **11**, 220 (1968).
- ²⁷J. A. Pople and G. A. Segal, *J. Chem. Phys.* **44**, 3289 (1966).